PCCP

Accepted Manuscript

ROYAL SOCIETY OF CHEMISTRY

www.rsc.org/pccp

DIRECTOR ALIGNMENT RELATIVE TO THE TEMPERATURE GRADIENT IN NEMATC LIQUID CRYSTALS STUDIED BY MOLECULAR DYNAMICS SIMULATION

Sten Sarman
Department of Materials and Environmental Chemistry
Arrhenius Laboratory
Stockholm University
106 91 Stockholm
Sweden
and
Aatto Laaksonen*
Stellenbosch Institute of Advanced Studies (STIAS),
Wallenberg Research Centre at Stellenbosch University,
Marais Street, Stellenbosch 7600
South Africa

* Permanent address
Department of Materials and Environmental Chemistry
Arrhenius Laboratory
Stockholm University
106 91 Stockholm
Sweden

Abstract

The director alignment relative to the temperature gradient in nematic liquid crystal model systems consisting of soft oblate or prolate ellipsoids of revolution has been studied by molecular dynamics simulation. The temperature gradient is maintained by thermostatting different parts of the system at different temperatures by using a Gaussian thermostat. It is found that the director of the prolate ellipsoids aligns perpendicular to the temperature gradient whereas the director of the oblate ellipsoids aligns parallel to this gradient.

When the director is oriented in between the parallel and perpendicular orientation a torque is exerted forcing the director to the parallel or perpendicular orientation. Because of symmetry restrictions there is no linear dependence of the torque being a pseudovector on the temperature gradient being polar vector in an axially symmetric system such as a nematic liquid crystal. The lowest possible order of this dependence is quadratic. Thus the torque is very weak when the temperature gradient is small, which may explain why this orientation phenomenon is hard to observe experimentally. In both cases the director attains the orientation that minimises the irreversible entropy production.

1. Introduction

Many technological applications of liquid crystals are based on their ability to orient relative to external fields, such as electric and magnetic fields. They also orient relative dissipative fields such as velocity gradients and temperature gradients [1, 2]. However, the orientation caused by the last-mentioned field has been considerably less studied. The reason for this is probably that it is hard to observe because there is no linear coupling between the temperature gradient being a polar vector and a possible orienting torque being pseudovector in an axially symmetric system such as a nematic liquid crystal. The lowest possible order of the coupling allowed by the symmetry is quadratic in the temperature gradient and consequently it will be very weak if the temperature gradient is small. Note, however, that a linear coupling is allowed in a cholesteric liquid crystal, where a temperature gradient parallel to the cholesteric axis induces a torque rotating the director.

The first experimental study of a nematic liquid crystal orienting relative to a temperature gradient was reported by Stewart in 1936 [3], who found that the director attained the perpendicular orientation relative to this gradient. This study was then confirmed in a series of papers [4-6] by Holland, Stewart and Reynolds, who also ruled out that the orientation phenomena were due to convection. Later on in the 1960's Picot and Fredrickson [7] and Fisher and Fredrickson [8] doubted that any orientation phenomena caused by temperature gradients actually existed in nematic liquid crystals while Patharkar, Rajan and Picot [9] provided some experimental results supporting the existence of such orientation phenomena. Curry [10] suggested that the phenomenon was due to convection. The possible coupling between the temperature gradient and the director orientation is also of interest in the study of the Bénard instability [11] and of various other convectional instabilities [12, 13] in nematic liquid crystals.

In a simulation study in the mid 1990's [14] the orientation of the director relative to a temperature gradient was examined in two molecular liquid crystal model systems consisting of soft prolate and oblate ellipsoids of revolution, respectively. It was found that the director of a nematic liquid crystal consisting of the prolate ellipsoids oriented perpendicularly to the temperature gradient and that the director of the oblate ellipsoids oriented parallel to this gradient. If the director was fixed in another orientation between the parallel and perpendicular orientations, a torque was exerted on the director forcing it to the parallel or perpendicular orientation. However, the effects of the temperature gradient were created by applying non-Newtonian synthetic equations motion that included a fictitious mechanical heat field driving a heat current without any actual temperature gradient. The field was designed in such a way

that the zero field limit of the ratio of heat current and the field coincided with the value of the corresponding Green-Kubo relation [15, 16] for the heat conductivity. Unfortunately, the mechanical field included an additional torque acting on the molecules, so that it is not impossible that the observed orientation phenomena were caused by this torque rather than being a real effect of a temperature gradient. Therefore, the purpose of the present work is to maintain a temperature gradient driving a heat current in the liquid crystal system in a more realistic way by thermostatting different regions of the system at different temperatures. Only the translational degrees of freedom will be thermostatted, so that the thermostatting mechanism itself does induce any torques that could affect the director orientation. Between the thermostatted regions the equations of motion will be more or less Newtonian. Thus it will be possible to unambiguously determine whether there is a coupling between the temperature gradient and an orienting torque.

The article is organized as follows: in section 2 the necessary theory is reviewed, in section 3 the model system is described, in section 4 some technical details are given, in section 5 the results are presented and discussed and finally in section 6 there is a conclusion.

2. Theory

2.1 Order parameter, director and director angular velocity

The order parameter S of a nematic liquid crystal consisting of axially symmetric molecules is defined as the largest eigenvalue of the order tensor

$$\mathbf{Q}^{uu} = \frac{3}{2}\left(\frac{1}{N}\sum_{i=1}^{N}\hat{\mathbf{u}}_i'\hat{\mathbf{u}}_i' - \frac{1}{3}\mathbf{1}\right), \tag{1}$$

where $\hat{\mathbf{u}}_i$ is the axis vector of molecule i, $\mathbf{1}$ is the second rank unit tensor and N is the number of molecules. When the order parameter is equal to zero, the orientation of the molecules is completely random and when it is equal to one the molecules are perfectly aligned. The eigenvector corresponding to the largest eigenvalue is called the director, **n**, and it is a measure of the average orientation of the molecules. The orientations **n** and **-n** are equivalent. The order tensor can be expressed in terms of the order parameter and the director,

$$\mathbf{Q} = \frac{3}{2}S\left(\mathbf{nn} - \frac{1}{3}\mathbf{1}\right). \tag{2}$$

The director angular velocity is given by $\boldsymbol{\Omega} = \mathbf{n} \times \dot{\mathbf{n}}$. Since the simulation cell is very small compared to a real system there is only one director and one director angular velocity for the whole system.

2.2 Macroscopic phenomenological relations

In an axially symmetric system such as a nematic liquid crystal a temperature gradient drives a heat current [1, 2, 16],

$$\left\langle \mathbf{J}_Q \right\rangle = -[\lambda_{\parallel\parallel}\mathbf{nn} + \lambda_{\perp\perp}(\mathbf{1} - \mathbf{nn})] \cdot \frac{\boldsymbol{\nabla} T}{T}, \tag{3}$$

where $\left\langle \mathbf{J}_Q \right\rangle$ is the heat current density, $\mathbf{n}$ is the director , T is the absolute temperature, $\boldsymbol{\nabla} T$ is the temperature gradient, $\lambda_{\parallel\parallel}$ is the heat conductivity in the direction parallel to the director and $\lambda_{\perp\perp}$ is the heat conductivity perpendicular to the director. The angular brackets denote that the heat current density is the ensemble average of a phase function. The temperature gradient is a polar vector that drives a heat current being another polar vector. In isotropic systems or axially symmetric systems, the symmetry forbids linear couplings between thermodynamic forces and fluxes that are polar vectors and pseudo vectors, respectively [16]. Thus a linear coupling between a temperature gradient and an orienting torque is excluded. However, it is possible to have a cross coupling between a second rank symmetric tensor and a pseudovector in an axially symmetric system. Such a tensor can be obtained by forming a dyadic product of the temperature gradient. Then the coupling between the temperature gradient and the torque density up to quadratic order can be written as (14):

$$\left\langle \boldsymbol{\Gamma}_{\nabla T} \right\rangle / V = \mu \boldsymbol{\varepsilon} : \left(\mathbf{nn} \cdot \frac{\boldsymbol{\nabla} T}{T} \frac{\boldsymbol{\nabla} T}{T} \right) = \mu \mathbf{n} \cdot \frac{\boldsymbol{\nabla} T}{T} \mathbf{n} \times \frac{\boldsymbol{\nabla} T}{T}, \tag{4}$$

where μ is a cross coupling coefficient, $\boldsymbol{\varepsilon}$ is the Levi-Civita tensor and V is the volume of the system. The torque is zero in the parallel and perpendicular orientations but finite in any other orientation, thus forcing the director to either of these orientations. It is consequently possible for a temperature gradient to orient the director. However, the torque becomes proportional to the square of the temperature gradient, so that it will be very weak when the temperature gradient is small.

2.3 Microscopic theory: heat flow algorithm and equations of motion

In a real system the heat flow is driven by a temperature gradient that arises because there are different temperatures in different regions of the system. In the simulation cell this can be achieved by keeping one region in the system at a high temperature T_2 and another region at a low temperature T_1, so that heat flows from the hot region to the cold region, see fig. 1. Then the heat conductivity is obtained by dividing the heat current by the temperature gradient. A molecular dynamics algorithm for calculating the heat conductivity in this way was devised by Ikeshoji and Hafskjold [17] in 1994 and a variant of this algorithm will be applied in this work. Mathematically, the different temperatures are obtained by constraining the kinetic energy to attain different values in the two regions. In order to avoid sharp boundaries of the regions and thereby numerical problems when the equations of motion are integrated, the temperature is allowed to vary continuously by weighting the kinetic energy of the particles according to their position. Therefore two weight functions are introduced,

$$W_{vi} = \exp[-(z_i - z_v)^2] / 2a^2 , \tag{5}$$

where z_i is the *z*-coordinate of particle *i* and z_v, v = 1, 2, is the *z*-coordinate of region 1 and 2, respectively, $z_1 = l/4$, $z_2 = 3l/4$, *l* is the length of the simulation cell in the *z*-direction and the parameter *a* is a decay length. The actual function selected for the weight functions is rather arbitrary; any well-behaved function can be applied. In order to simplify the algebra the normalized weight functions are used,

$$w_{vi} = W_{vi} \Big/ \sum_{j=1}^{N} W_{vj} \ . \tag{6}$$

The following two constraints of the weighted translational kinetic energy per particle are applied,

$$\frac{1}{2} \sum_{j=1}^{N} w_{vj} m \dot{\mathbf{r}}_j^2 - K_v = 0 , \tag{7}$$

where *v* is equal to 1 or 2, *m* is the mass of the particles and $\dot{\mathbf{r}}_j$ is the velocity of particle *j*, and K_v is the translational kinetic energy per particle. If K_1 and K_2 are given different values the temperatures at z_1 and z_2 will be different. Provided that *l* is long compared to the decay length *a* of the weight functions these two constraint do not disturb each other and the equations of motion between the thermostatted regions will be essentially Newtonian. Only the translational kinetic energy is constrained whereas the rotational kinetic energy is left free in order not to interfere with the angular degrees of freedom and thereby influencing the orienta-

tion of the molecules and thereby the director. Equations of motion satisfying these constraints can be obtained by applying Gauss's principle of least constraint [15]. Then the constraints must be expressed in terms of the accelerations, which can be done by differentiating the above constraint equations (7) with respect to time,

$$\sum_{i=1}^{N} m\left(w_{vj}\dot{\mathbf{r}}_j \cdot \ddot{\mathbf{r}}_j + \frac{1}{2}\dot{w}_{vj}\dot{\mathbf{r}}_j^2 \right) = 0 . \tag{8}$$

In order to conserve the linear momentum, the constraint

$$\sum_{i=1}^{N} m\ddot{\mathbf{r}}_j = \mathbf{0} \tag{9}$$

is also applied. Note that this is a vector constraint, where the three components of the linear momentum are kept constant independently of each other. According to Gauss's principle, the equations of motion are obtained by minimizing a quantity known as the square of the curvature *C*,

$$C = \frac{1}{2}\sum_{j=1}^{N} m\left(\ddot{\mathbf{r}}_j - \frac{\mathbf{F}_j}{m} \right)^2 , \tag{10}$$

where $\mathbf{F}_j$ is the force exerted on particle *j* by the other particles, with respect to the acceleration subject to the above constraints,

$$\frac{\partial}{\partial \ddot{\mathbf{r}}_i}\left\{ C + \alpha_1 \sum_{j=1}^{N} m\left(w_{1j}\dot{\mathbf{r}}_j \cdot \ddot{\mathbf{r}}_j - \frac{1}{2}\dot{w}_{1j}\dot{\mathbf{r}}_j^2 \right) + \alpha_2 \sum_{j=1}^{N} m\left(w_{2j}\dot{\mathbf{r}}_j \cdot \ddot{\mathbf{r}}_j + \frac{1}{2}\dot{w}_{2j}\dot{\mathbf{r}}_j^2 \right) + \boldsymbol{\beta} \cdot \sum_{j=1}^{N} m\ddot{\mathbf{r}}_j \right\} = 0 , \tag{11}$$

where α_1, α_2 and $\boldsymbol{\beta}$ are constraint multipliers, whereby the following equations of motion are obtained,

$$m\ddot{\mathbf{r}}_i = \mathbf{F}_i - \alpha_1 m\left(w_{1i}\dot{\mathbf{r}}_i - \frac{1}{N}\sum_{j=1}^{N} w_{1j}\dot{\mathbf{r}}_j \right) - \alpha_2 m\left(w_{2i}\dot{\mathbf{r}}_i - \frac{1}{N}\sum_{j=1}^{N} w_{2j}\dot{\mathbf{r}}_j \right), \tag{12}$$

after elimination of the momentum constraint multiplier $\boldsymbol{\beta}$. The values of the multipliers α_1 and α_2 are determined by insertion of the accelerations in the constraint equations (8). Note that Gauss's principle in the absence of constraints gives the ordinary Newtonian equations of motion and that it is identical to Lagrange's method for holonomic constraints, *i.e.* constraints that only depend on the coordinates. However, Gauss's principle is more general in that it in addition to holonomic constraints also allows some constraints involving both velocities and coordinates.

When these equations of motion are applied, there is no net heat current in the system. However, the heat current can be obtained from the rate of change of the internal energy,

$$\left\langle \dot{E} \right\rangle = \left\langle \sum_{i=1}^{N} \left(m\dot{\mathbf{r}}_i \cdot \ddot{\mathbf{r}}_i - \mathbf{F}_i \cdot \dot{\mathbf{r}}_i \right) \right\rangle = -\left\langle \alpha_1 m \sum_{i=1}^{N} w_{1i} \dot{\mathbf{r}}_i^2 \right\rangle - \left\langle \alpha_2 m \sum_{i=1}^{N} w_{2i} \dot{\mathbf{r}}_i^2 \right\rangle = 0 , \tag{13}$$

the average of which is equal to zero in a steady state. Then the first term on the right hand side being equal to the rate of energy removed in the cold region and the second term being equal the rate of energy supplied in the hot region cancel out in a steady state. Since the heat current density is defined as the energy flow per unit area, its *z*-component perpendicular to the hot and cold regions becomes:

$$AJ_{Qz} = -\frac{1}{2}\left\langle \alpha_1 m \sum_{i=1}^{N} w_{1i} \dot{\mathbf{r}}_i^2 \right\rangle = -\frac{1}{2}\left\langle \alpha_2 m \sum_{i=1}^{N} w_{2i} \dot{\mathbf{r}}_i^2 \right\rangle , \tag{14}$$

where A is the cross sectional area of the simulation cell and the factor of ½ arises because the heat flows in two directions from the hot to the cold region. From this relation it is possible to calculate the heat conductivity by dividing the heat current by the temperature gradient,

$$\lambda = \frac{J_{Qz}}{(T_2 - T_1)/(l/2)} . \tag{15}$$

Note, however, that this heat conductivity is the average of the heat conductivity for the temperatures between T_1 and T_2, so that it must be linearly dependent on the temperature and the temperature profile must by linear if this expression is to yield accurate results. In general the conventional methods such as Green-Kubo relations [15, 16] and the Evans heat flow algorithm [15] are more accurate and easier to implement.

In angular space the ordinary Euler equations are applied,

$$\mathbf{I}_p \cdot \dot{\boldsymbol{\omega}}_{pi} = -\boldsymbol{\omega}_{pi} \times \mathbf{I}_p \cdot \boldsymbol{\omega}_{pi} + \boldsymbol{\Gamma}_{pi} , \tag{16}$$

where $\boldsymbol{\omega}_{pi}$ is the angular velocity and $\mathbf{I}_p$ is the inertia tensor, $\boldsymbol{\Gamma}_{pi}$ is the torque exerted on molecule i by the other molecules and the subscript 'p' denotes the principal frame. The relation between the molecular angular velocities and the rate of change of the axis vectors $d\hat{\mathbf{u}}_i / dt$ is expressed in terms of quaternions [18].

It is also interesting to determine whether a torque is acting on the director when it is oriented at an angle between the parallel and perpendicular orientation relative to the temperature gradient. This can be achieved by fixing the director in a specified direction by adding two Lagrangian constraint torques that force the director angular velocity to be zero [14, 19],

$$\mathbf{I}_p \cdot \dot{\boldsymbol{\omega}}_{pi} = -\boldsymbol{\omega}_{pi} \times \mathbf{I}_p \cdot \boldsymbol{\omega}_{pi} + \boldsymbol{\Gamma}_{pi} + \gamma_y \frac{\partial \Omega_y}{\partial \boldsymbol{\omega}_{pi}} + \gamma_z \frac{\partial \Omega_z}{\partial \boldsymbol{\omega}_{pi}}, \tag{17}$$

where Ω_y and Ω_z are the *y*- and *z*-components of the director angular velocity, γ_y and γ_z are Lagrangian constraint multipliers determined by the constraint that the director angular acceleration be zero. Thereby the director angular velocity remains constant and if it is equal to zero initially it will remain zero for all subsequent times whereby the director will be fixed in space. It has been shown that these constraints do not affect the ensemble averages of phase functions and time correlation functions provided that they do not involve the director angular velocity [20]. The constraint torque $\langle \boldsymbol{\Gamma}_{const} \rangle$ that arises when equation (17) is used balances the torque exerted by the temperature gradient $\langle \boldsymbol{\Gamma}_{\nabla T} \rangle$, *i.e.*

$$\langle \boldsymbol{\Gamma}_{const} \rangle = \left\langle \gamma_y \frac{\partial \Omega_y}{\partial \boldsymbol{\omega}_{pi}} + \gamma_z \frac{\partial \Omega_z}{\partial \boldsymbol{\omega}_{pi}} \right\rangle = -\langle \boldsymbol{\Gamma}_{\nabla T} \rangle, \tag{18}$$

and if we let the *z*-component of the director be zero we have [19]

$$\langle \boldsymbol{\Gamma}_{const} \rangle = -\langle \boldsymbol{\Gamma}_{\nabla T} \rangle = \left\langle \gamma_y \frac{\partial \Omega_y}{\partial \boldsymbol{\omega}_{pxi}} \right\rangle = \langle \gamma_y \rangle = 2V \langle P_y^a \rangle, \tag{19}$$

where P_y^a is the *y*-component of the antisymmetric part of the pressure tensor, which is equal to the external torque density, and the pressure tensor is given by the Irving and Kirkwood expression [21],

$$\langle \mathbf{P} \rangle V = \left\langle \sum_{i=1}^{N} \left(\frac{\mathbf{p}_i \mathbf{p}_i}{m} - \mathbf{r}_i \mathbf{F}_i \right) \right\rangle = \left\langle \sum_{i=1}^{N} \frac{\mathbf{p}_i \mathbf{p}_i}{m} - \sum_{i=1}^{N} \sum_{j=i+1}^{N} \mathbf{r}_{ij} \mathbf{F}_{ij} \right\rangle, \tag{20}$$

where $\mathbf{p}_i$ is the linear momentum of particle *i*, $\mathbf{r}_{ij}$ is equal to $\mathbf{r}_j - \mathbf{r}_i$ and $\mathbf{F}_{ij}$ is the force exerted on particle *i* by particle *j*.

In order to cross check the heat flow algorithm (12-15) and to determine its efficiency and accuracy it is useful to compare its estimates of the heat conductivity with those obtained by the conventional Green-Kubo relation,

$$\lambda_{\alpha\alpha} = \frac{V}{k_B T^2} \int_0^\infty dt \left\langle J_{Q\alpha}(t) J_{Q\alpha}(0) \right\rangle_{eq}, \tag{21}$$

where the subscript α denotes the parallel ($\|$) or perpendicular orientation ($\perp$) of the director relative to the temperature gradient and the subscript *eq* denotes that the time correlation function is evaluated in an equilibrium ensemble. The heat current of a system consisting of rigid bodies is given by [22],

$$V\left\langle \mathbf{J}_Q \right\rangle = \frac{1}{2}\left\langle \sum_{i=1}^{N} \frac{\mathbf{p}_i}{m}\left(\frac{\mathbf{p}_i^2}{m} + \cdot\boldsymbol{\omega}_{pi} \cdot \mathbf{I}_p \cdot \boldsymbol{\omega}_{pi} + \sum_{j=1, j\neq i}^{N} \Phi_{ij} \right) - \sum_{i}^{N} \sum_{j=1, j\neq i}^{N} \mathbf{r}_{ij}\left(\frac{\mathbf{p}_i}{m} \cdot \mathbf{F}_{ij} + \boldsymbol{\omega}_{pi} \cdot \boldsymbol{\Gamma}_{pij} \right) \right\rangle, \qquad (22)$$

where Φ_{ij} is the pair interaction energy between particle *i* and *j*, $\mathbf{r}_{ij}$ is equal to $\mathbf{r}_j - \mathbf{r}_i$, $\mathbf{F}_{ij}$ and $\boldsymbol{\Gamma}_{pij}$ are the force and torque exerted on particle *i* by particle *j*.

3. Model system

We have studied two different systems consisting of prolate or calamitic soft ellipsoids of revolution and oblate or discotic soft ellipsoids of revolution, respectively. The ellipsoids interact via a variant of the Gay-Berne potential [14, 23-25], where the Lennard-Jones core has been replaced by a purely soft repulsive $1/r^{18}$ potential,

$$U_{GB}(\mathbf{r}_{12}, \hat{\mathbf{u}}_1, \hat{\mathbf{u}}_2) = 4\varepsilon(\hat{\mathbf{r}}_{12}, \hat{\mathbf{u}}_1, \hat{\mathbf{u}}_2)\left[\frac{\kappa\sigma_0}{r_{12} - \sigma(\hat{\mathbf{r}}_{12}, \hat{\mathbf{u}}_1, \hat{\mathbf{u}}_2) + \kappa\sigma_0} \right]^{18}, \qquad (23)$$

where $\mathbf{r}_{12}$ is the distance vector between the centre of symmetry of molecule 1 and the centre of symmetry of molecule 2, $\hat{\mathbf{u}}_1$ and $\hat{\mathbf{u}}_2$ are the axis vectors of these molecules consisting of ellipsoids of revolution and σ_0 is the length of the axis perpendicular to the axis of revolution, *i.e.* the short axis of the prolate ellipsoids and the long axis of the oblate ellipsoids.

The strength and range parameters, $\varepsilon(\hat{\mathbf{r}}_{12}, \hat{\mathbf{u}}_1, \hat{\mathbf{u}}_2)$ and $\sigma(\hat{\mathbf{r}}_{12}, \hat{\mathbf{u}}_1, \hat{\mathbf{u}}_2)$ are given by

$$\varepsilon(\hat{\mathbf{r}}_{12}, \hat{\mathbf{u}}_1, \hat{\mathbf{u}}_2) = \varepsilon_0\left[1 - \chi^2(\hat{\mathbf{u}}_1 \cdot \hat{\mathbf{u}}_2)^2\right]^{-1/2} \times$$

$$\cdot\left\{1 - \frac{\chi'}{2}\left[\frac{(\hat{\mathbf{r}}_{12} \cdot \hat{\mathbf{u}}_1 + \hat{\mathbf{r}}_{12} \cdot \hat{\mathbf{u}}_2)^2}{1 + \chi' \hat{\mathbf{u}}_1 \cdot \hat{\mathbf{u}}_2} + \frac{(\hat{\mathbf{r}}_{12} \cdot \hat{\mathbf{u}}_1 - \hat{\mathbf{r}}_{12} \cdot \hat{\mathbf{u}}_2)^2}{1 - \chi' \hat{\mathbf{u}}_1 \cdot \hat{\mathbf{u}}_2} \right]\right\}^2 \qquad (24a)$$

and

$$\sigma(\hat{\mathbf{r}}_{12}, \hat{\mathbf{u}}_1, \hat{\mathbf{u}}_2) = \sigma_0\left\{1 - \frac{\chi}{2}\left[\frac{(\hat{\mathbf{r}}_{12} \cdot \hat{\mathbf{u}}_1 + \hat{\mathbf{r}}_{12} \cdot \hat{\mathbf{u}}_2)^2}{1 + \chi \hat{\mathbf{u}}_1 \cdot \hat{\mathbf{u}}_2} + \frac{(\hat{\mathbf{r}}_{12} \cdot \hat{\mathbf{u}}_1 - \hat{\mathbf{r}}_{12} \cdot \hat{\mathbf{u}}_2)^2}{1 - \chi \hat{\mathbf{u}}_1 \cdot \hat{\mathbf{u}}_2} \right]\right\}^{-\frac{1}{2}}, \qquad (24b)$$

where ε_0 is the depth of the potential minimum in the orientation where $\mathbf{r}_{12}$, $\hat{\mathbf{u}}_1$ and $\hat{\mathbf{u}}_2$ are mutually perpendicular, *i.e.* the cross configuration, χ is equal to $(\kappa^2 - 1)/(\kappa^2 + 1)$, where κ, denoting the ratio of the axis of revolution and the axis perpendicular to this axis, has been set equal to 3 for the prolate ellipsoids and to 1/3 for the oblate ellipsoids, the parameter χ' is

equal to $(\kappa'^{1/2}-1)/(\kappa'^{1/2}+1)$, where κ', denoting the ratio of the potential well depths of the side-by-side and end-to-end configurations of the prolate ellipsoids and the ratio of the edge-to-edge and the face-to-face configurations of the oblate ellipsoids, has been set equal to 5 in the first case and to 1/5 in the second case. Note that a purely repulsive potential is used, so there are no potential minima but the values optimised for the Lennard-Jones potential have been retained.

4. Technical details

The results are expressed in reduced units for the length, density, mass, energy, time and temperature equal to σ_0, σ_0^{-3}, m, ε_0, $t_0^* = \sigma_0(m/\varepsilon_0)^{1/2}$ and ε_0 / k_B where k_B is Boltzmann's constant. The equations of motion were integrated by using a fourth order Gear predictor-corrector method with a timestep of $0.001\, t_0^*$ for the prolate ellipsoids and $0.0005\, t_0^*$ for the oblate ellipsoids. Cutoff radii of $4.5\,\sigma_0$ and $2.0\ \sigma_0$ beyond which the pair interaction potential was set equal to zero were applied for the prolate and oblate ellipsoids, respectively. A cell code was used to accelerate the formation of the neighbour list.

In order to cancel the numerical drift of the temperature and director constraints arising because the numerical methods used to integrate the equations of motion never are completely exact, proportional feedback multipliers [26] were used. Then the actual values used of the thermostatting multipliers α_1 and α_2 are

$$\alpha_\nu' = \alpha_\nu - \zeta_\nu \left(\frac{1}{2} \sum_{j=1}^{N} w_{\nu j} m \dot{\mathbf{r}}_j^2 - K_\nu \right), \tag{25}$$

where $\nu = 1, 2$ and ζ_ν is a feedback multiplier. In the same way, the director constraint multipliers in equation (17) were augmented by proportional feedback multipliers [14], *i. e.*

$$\gamma_y' = \gamma_y - \xi_y \Omega_y + \eta_z (n_z - n_{0z}) \tag{26a}$$

and

$$\gamma_z' = \gamma_z - \xi_z \Omega_z - \eta_y (n_y - n_{0y}), \tag{26b}$$

where vξ_y, ξ_z, η_y and η_z are feedback multipliers, Ω_y and Ω_z are the y- and z-components of the director angular velocity, n_y and n_z are the actual values of the y- and z-components of the director and n_{0y} and n_{0z} are the corresponding desired values. If the numerical integration method of the equations of motion were exact the constraints would be exactly satisfied and

the expressions within the brackets and Ω_y and Ω_z would be exactly zero, so that $\alpha_\nu' = \alpha_\nu$, $\gamma_y' = \gamma_y$ and $\gamma_z' = \gamma_z$. If the proportional feedback multipliers are given values of between 0.1 and 10 in reduced units there will be very small deviations, *i.e.* relative errors of the order of 10^{-7} or less, that will have negligible influence on the ensemble averages of the phase functions and time correlation functions. In the present calculations the ζ_ν's were equal to 1.0 and ξ_y, ξ_z, η_y and η_z were equal to 0.1.

Some of the conclusions in this work are based on angular distribution functions $p(\theta)$ of the director relative to the temperature gradient, where θ is the angle between the director and the temperature gradient. In the simulation these functions are obtained in the following way: Every fifth time step of the simulation run, the angle θ between the director and the temperature gradient is calculated. Then an array element with an index equal to the integer part of the calculated value of θ in degrees is increased by one. Thus the total array becomes a histogram of a sampling of the distribution function $p(\theta)\sin\theta$. This sampling is linear in θ. By dividing by the factor $\sin\theta$ the angular distribution function $p(\theta)$ is recovered.

5. Calculations, results and discussion

The first step that must be carried out is to verify that it is possible to use the heat flow algorithm (12-15) to obtain estimates of the heat conductivity that are consistent with those obtained by evaluation of the conventional equilibrium Green-Kubo relation (21). Therefore a calamitic system consisting of 8192 prolate ellipsoids at a reduced density $n^*= n\sigma_0^3$ of 0.30 in a cubic box with a length of $30\,\sigma_0$ was studied. The thermostats were located at z_1=7.5 σ_0 and z_2=22.5 σ_0 and the decay length a of the Gaussian weight functions (5) was given a value of 1.00 σ_0. The reduced temperatures T_1 and T_2 were set equal to 0.95 and 1.05, respectively. Note that even though the temperature gradient orients the director it will fluctuate around the preferred orientation and then the calculated heat conductivity becomes the average over a rather wide angular interval. When the heat conductivity in the direction that is not preferred is calculated the director is forced away from this direction. Therefore, the constraint equations (17) were applied to fix the director either parallel or perpendicularly to the temperature gradient. The resulting translational temperature profile of the calamatic system where the director is parallel to the temperature gradient is shown in fig. 2, where it can be seen that the profile is more or less linear. According to the equipartition principle the translational and

rotational temperatures are the same at equilibrium but this is not necessarily the case away from equilibrium. Here these two temperatures agree with each other within relative errors of 0.005 or less even though only the translational degrees of freedom were thermostatted. The relative difference between the total translational and total rotational kinetic energies of the whole system is about 0.0002. When the temperature difference is increased by setting T_1 and T_2 equal to 1.00 and 2.00, the largest relative difference between the rotational and kinetic temperatures is less than 0.025 and the relative difference between the corresponding total energies for the whole system is about 0.0005. The translational and rotational temperature profiles for the perpendicular orientation are similar to the displayed profile. Since the temperature profile is more or less linear, the temperature gradient can be approximated rather accurately by the difference between the high and low temperatures divided by the distance between the hot and cold regions. It is found that the maximal temperature $T_{\max}$ is somewhat higher than T_2 and that the minimal temperature $T_{\min}$ is somewhat lower than T_1. This is not inconsistent because the constraints only require that the averages of the temperatures within the range of the weight functions should be equal to T_1 and T_2. Consequently, a slightly more accurate value of the temperature gradient is obtained by using the expression $(T_{\max} - T_{\min}) / (l / 2)$ rather than $(T_2 - T_1) / (l / 2)$. Then the heat conductivity is calculated by dividing the rate of change of the internal energy obtained from equation (14) by the temperature gradient and the cross sectional area of the simulation cell. The estimates of heat conductivity are compared to the Green-Kubo estimates of equation (21) in table 1 and it turns out that the relative difference is less than 5 percent, which is surprisingly accurate not least when it is taken into account that these nonequilibrium simulations are four times shorter (4×10^3 t_0^*) than the equilibrium simulations (1.6×10^4 t_0^*) used to evaluate the Green-Kubo relations.

The heat flow algorithm was also verified for a discotic system consisting of 8192 oblate ellipsoids, at reduced density of n^* of 2.4 in a cubic box with a box length of $15\,\sigma_0$. The thermostats were located at $z_1 = 3.75\,\sigma_0$ and $z_2 = 11.25\,\sigma_0$ and the decay length a of the Gaussian weight functions (5) was equal to $0.5\ \sigma_0$. The reduced translational temperatures were set equal to 0.95 and 1.05 respectively as in the previous case. The temperature profile was found to be virtually linear and the translational and rotational temperature profiles coincided within relative errors of less than 0.003. The relative difference between the corresponding energies of the whole system was about 0.0005. The comparison with the Green-Kubo

estimates is given in table 1. The relative error is less than 10 percent. Thus we can be confident that the heat flow algorithm (12-15) gives a more or less linear temperature gradient and that the heat conduction follows Fourier's law.

The second step is the principal topic of this work, namely to examine how the director of a nematic liquid crystal orients relative to the temperature gradient. It could be thought that this would be impossible to determine with the present arrangement of thermostats because there are two temperature gradients in opposite directions in the system, see fig. 1 and fig. 2 and that the director therefore would be twisted in different directions in either half of the system. However, since the torque induced by the temperature gradient is proportional to the square of this gradient or is at least an even function of the gradient because of symmetry, see equation (4), it remains the same when the gradient changes sign and thus it is the same in the whole system, so that the director is twisted in the same direction in both halves of the system.

The most immediate way to examine whether the temperature gradient affects the orientation of the director is to calculate its angular distribution, $p(\theta)$, relative to this gradient. This function, obtained according to the method described in section 5, is displayed in figure 3 at two state points of the calamitic system, where the two temperatures T_1 and T_2 were equal to 1.00 and 1.50 at the first state point and to 1.00 and 1.25 at the second one and the run length was $1.5 \times 10^6\ t_0^*$. As it can be seen, the angular distribution of the director is more or less Gaussian in both cases and the maximum is located around the 90 degree orientation or the perpendicular orientation. Thus the perpendicular orientation is the preferred orientation. The distribution function becomes narrower when the temperature gradient increases because a larger gradient induces a larger torque that more efficiently counteracts the spontaneous thermal fluctuations of the director out of the perpendicular alignment. These distribution functions were compared to the corresponding function of the discotic system, where T_1 and T_2 were equal to 1.00 and 1.50 and the run length was equal to $1 \times 10^6\ t_0^*$. The angular distribution function is displayed in fig. 4. In contrast to the previous systems the distribution function here is maximal at the zero degree orientation or the parallel orientation. In this case it is more difficult to obtain accurate values of $p(\theta)$ since it is actually a histogram corresponding to $p(\theta)\sin\theta$ that is calculated and this function goes to zero as θ goes to zero, so that the statistics becomes very poor for small values of θ. However, still an approximately Gaussian angular distribution is obtained.

These distribution functions imply that the temperature gradient forces the director of the calamitic system towards the perpendicular orientation whereas the gradient forces the director of the discotic system towards the parallel orientation. The angular distributions of the director are rather wide since the systems are very small and thus the thermal fluctuations are very large. However, in the thermodynamic limit these fluctuations decrease and the widths of the distributions go to zero.

In order to rule out that the director orientation could be affected by the initial conditions or by the periodic boundary conditions the simulations were started from a crystal configuration that was allowed to melt during a time period of 500 t_0^* which should be enough to form a nematic liquid crystal. Then the temperature gradient was applied both parallel and perpendicularly to the director and it was found that the director of the calamitic system in both cases attained the perpendicular orientation. In the same way the director of the discotic system attained the parallel orientation independently of the initial orientation. Moreover, the director is not statically fixed in the parallel or perpendicular orientation, but it fluctuates around these orientations with very large amplitudes, *i.e.* 30 degrees or more, so that it is not locked by the initial configuration. It is also possible that the system size and the period boundary conditions could influence the director orientation. This is a problem when smectic phase are studied because then a stress arises if the length of the simulation box is not an integer multiple of the layer spacing. However, this is less of a problem in the nematic phase that was simulated in the present work, since there is only orientational order but no translational order. In addition the systems are very large, *i.e.* the length of the simulation cell is equal to 10 molecular lengths in the calamitic system and to 15 molecular diameters in the discotic system. Finally, a great deal of experience on simulation of rotation and tumbling of nematic liquid crystal model systems in order to obtain the twist viscosity has been accumulated, see refs. [19, 27, 28] and the general conclusion is that the periodic boundary conditions do not affect the rotation to any greater extent.

In order to further confirm these results on the director orientation and to provide additional evidence for that the orientation is independent of the initial conditions, the constraint algorithm (17) was used to fix the director at given angles relative to the temperature gradient to calculate the exerted torque $\langle \mathbf{\Gamma}_{\nabla T} \rangle$ (18, 19) as a function of the orientation angle. In these calculations the director is confined to the *zx*-plane, the temperature gradient is applied in the *z*-direction and a possible torque is exerted on the director around the *y*-axis, see fig. 5. Then a

positive torque twists the director clockwise towards the perpendicular orientation and a negative torque twists the director counter clockwise towards the parallel orientation. In this geometry the dependence of the torque on the director orientation angle θ and the temperature gradient (4) becomes:

$$\left\langle \Gamma_{\nabla Ty} \right\rangle / V = \mu \sin 2\theta \left(\frac{\partial_z T}{T} \right)^2 . \qquad (27)$$

In figs. 6a and 6b the torque density $\left\langle \Gamma_{\nabla Ty} \right\rangle / V$ is shown as a function of the angle between the director and the temperature gradient for the calamitic system at the same state points as above, *i.e.* the two temperatures T_1 and T_2 were equal to 1.00 and 1.50 at the first state point and to 1.00 and 1.25 at the second one. Run lengths of 1.2×10^5 t_0^* and 1×10^6 t_0^* were used for the large and small gradients, respectively. As it can be seen, the torque is clearly positive for all angles between 0 and 90°, so the director is twisted towards the perpendicular orientation at any other orientation even close to the parallel orientation. This provides further evidence that a temperature gradient forces the director of a calamitic nematic liquid crystal towards the perpendicular orientation independently of the initial orientation. The ratio of the maximal torque density and the temperature gradient in reduced units is about 0.1 for the large temperature gradient and 0.03 for the small temperature gradient. This is two orders of magnitude less than the heat conductivity, so the cross coupling is very weak.

According to equation (27) $\left\langle \Gamma_{\nabla Ty} \right\rangle$ should be a symmetric function of the orientation angle, proportional to $\sin 2\theta$ with a maximum at the 45 degree orientation. However, this does not seem to be the case, instead the absolute value of the torque is maximal at the 30 degree orientation and it falls off linearly towards the 90 degree orientation and in a more curved fashion towards the 0 degree orientation both in case of the large and the small temperature gradient. The torque should also be proportional to the square of the temperature gradient but this does not seem to be the case either. The reasons for this could be that the temperature gradients applied are too large, so that terms of higher order than quadratic become important. Had we applied smaller temperature gradients it might have been possible to observe a quadratic angularly symmetric dependence but this would have required prohibitively long simulation runs. Another factor that could contribute to the deviations from equation (27) is that the order parameter difference between the two temperatures is rather large, see table 2. However, the order parameters are still rather large, so the systems are far enough from the nematic-isotropic phase transition where fluctuations of these parameters could affect the di-

rector alignment. Note also that even though the change of the order parameter is rather large, this does not imply that the order parameter fluctuations are large, at least not far from the phase transitions points.

Also for the discotic system the torque density $\left\langle \Gamma_{\nabla Ty} \right\rangle / V$ was evaluated as a function of the orientation angle by applying the constraint algorithm (17) to fix the director. The state point was the same as the one above where the director angular distribution function was calculated, *i.e.* T_1 and T_2 were equal to 1.00 and 1.50. The results obtained from run lengths of 1×10^6 t_0^* are shown in fig. 7 where it can be seen that the torque now is negative for every angle between 0 and 90° even when the angle is close to 90° thus forcing the director towards the parallel orientation irrespective of the initial orientation. Also here the torque dependence on the orientation angle is nonsymmetrical around the 45 degree orientation. Instead, the maximum of the absolute value of the torque appears at the 60 degree orientation and the functional forms of the decay on either side of the maximum differ.

The ratio of the maximal torque density and the temperature gradient is only about 0.05 in reduced units, so the cross coupling must be regarded as very weak even in the discotic system studied. This ratio is likely to be even smaller in real systems because there the molecules are more irregular and the order parameter is lower and consequently the cross coupling coefficient μ in equations (4) and (27) become smaller, so that it will be very difficult to observe this orientation effect experimentally.

We finally observe that in both the calamitic system and the discotic system the director attains the orientation where the irreversible entropy production caused by the heat flow is minimal.

6. Conclusion

A heat flow was driven through two different liquid crystal model systems consisting of soft ellipsoids of revolution interacting according to a purely repulsive version of the Gay-Berne potential, one of which was a calamitic system composed of prolate ellipsoids of revolution and the other one was a discotic system composed of oblate ellipsoids of revolution. The heat flow was driven by applying a thermostat that kept one part of the system at a high temperature and another part at a low temperature, so that temperature gradient inducing a heat flow arose. The thermostat was based on a Gaussian constraint algorithm for the kinetic energy where a continuous and differentiable spatial weight function is used to constrain the

kinetic energy of the particles in a limited region in the system. If two such regions are introduced and they are far away from each other the kinetic energy can be constrained to different values in the two regions and thereby their temperatures become different so that a temperature gradient and a heat flow arise. It is possible to use the heat flow and the temperature gradient to calculate the heat conductivity even though the conventional Green Kubo methods or the Evans nonequilibrium molecular dynamics heat flow algorithm are more convenient to apply. However, the estimates of the heat conductivities for the liquid crystal model systems were found to agree very well the corresponding Green-Kubo estimates.

When the nematic phase of the liquid crystal model systems were subjected to the temperature gradient the director was oriented. It was found that the director of the calamitic system displayed an approximately Gaussian angular distribution function around the perpendicular orientation relative to the temperature gradient. On the other hand, the director of the discotic system was found to orient parallel to the temperature gradient, also with a more or less Gaussian angular distribution function. In order to verify these results, the director was fixed at different angles relative to the temperature gradient by applying a Lagrangian constraint torque that exactly cancels out any torque that is exerted on the director, in this case a torque exerted by the temperature gradient. In the calamitic system it was found that a torque twisting the director towards the perpendicular orientation was exerted by the temperature gradient when the director attains any other orientation. The torque was maximal around the 30 degree orientation, *i.e*. the torque was not symmetric around the 45 degree orientation. In the discotic system the director was found to be twisted towards the parallel orientation if it attained any other orientation relative to the temperature gradient. The torque was maximal around the 60 degree orientation. In both cases the torque was found to be very weak. The reason for this could be that a linear coupling between a temperature gradient being a polar vector and torque being a pseudo vector is forbidden because of symmetry restrictions; the lowest possible order is quadratic. Thus the torque becomes very weak if the temperature gradient is low. Even though very regular molecules that form liquid crystals with high order parameters compared to real liquid crystals were employed, the torques were very small and thus they are probably even smaller in real systems with more irregularly shaped molecules and lower order parameters, so that this could be one of the reasons why it is hard to observe experimentally. The results obtained confirm the results of an earlier work [14] where the Evans synthetic heat flow algorithm was used to drive the heat flow. Unfortunately, when that algorithm is used a mechanical heat field is applied where an explicit torque is exerted direct-

ly on the molecules. Thus it could not be ruled out that the orientation was caused by this field. However, no explicit torque is exerted when the heat flow algorithm (12-15) is applied, so that the orientation phenomena found in the present work can be unambiguously attributed to the temperature gradient. Finally we note that in both the calamitic system and the discotic system the director attains the orientation that minimizes the irreversible entropy production caused by the heat flow.

Acknowledgement

This work was supported by the Swedish National Infrastructure for Computing (SNIC) via PDC. One of us (AL) gratefully acknowledges support from Vetenskapsrådet (Swedish Research Council).

Figure Captions

Fig. 1

The thermostat arrangement. One region is kept at a high temperature and the other region is kept at a low temperature, so that heat flows from the hot region to the cold region orienting the director relative to the temperature gradient.

Fig. 2

The translational temperature profile (dotted curve) of a calamitic system where the director is kept perpendicular to the temperature gradient by application of the director constraint algorithm (17). The hot region is kept at a reduced temperature of 1.05 and the cold region at a temperature of 0.95. The full curves are the Gaussian weight functions (5).

Fig. 3

The angular distribution of the director, $p(\theta)$, of the calamitic liquid crystal, T_1 =1.00 and T_2 = 1.50 (filled circles) T_1 =1.00 and T_2 = 1.25 (open circles). The error bars are of the of same size as the symbols.

Fig. 4

The angular distribution of the director, $p(\theta)$, of the discotic liquid crystal, T_1=1.00 and T_2 = 1.50.

Fig. 5

The geometrical arrangement for the evaluation of the torque acting on the director. The temperature gradient points in the *z*-direction, the director **n** is constrained to the *zx*-plane at an angle θ to the z-axis and a possible induced torque is parallel to the *y*-axis.

Fig. 6a

The torque density, $\left\langle \Gamma_{\nabla Ty} \right\rangle / V$, acting on the director of the calamitic liquid crystal as a function of the angle relative to the temperature gradient, where T_1 = 1.00 and T_2 = 1.50.

Note that the torque density has been multiplied by a factor of 1 000. The error bars are of the same size as the symbols.

Fig. 6b

As in fig. 6a but T_1=1.00 and T_2 = 1.25.

Fig. 7

The torque density, $\left\langle \Gamma_{\nabla Ty} \right\rangle / V$, acting on the director of the discotic liquid crystal as a function of the angle relative to the temperature gradient, filled circles T_1 =1.00 and T_2 = 1.50. Note that the torque density has been multiplied by a factor of 1 000.

Table captions

Table 1

Comparison of the estimates of the heat conductivities obtained by the conventional Green-Kubo relations (lines 1 and 3) and those obtained by the nonequlibrium molecular dynamics algorithm, (12-15). The temperatures $T_{\max}$ and $T_{\min}$ are the maximal and minimal temperatures that have been used to evaluate the temperature gradient. The last column is the run length in reduced time units t_0^* that were used to obtain the results.

Table 2

The order parameter at the different temperatures for the calamitic and discotic systems.

Table 1

System	$\lambda_{\parallel\parallel}$	T_{max}	T_{min}	$\lambda_{\perp\perp}$	T_{max}	T_{min}	run length/ t_0^*
calamitic	9.5 ± 0.5			4.8 ± 0.3			1.6×10^4
	9.5 ± 0.1	1.054	0.947	5.0 ± 0.3	1.054	0.947	4×10^3
discotic	10.8 ± 0.8			31.5 ± 1.5			1.6×10^4
	11.8 ± 0.3	1.056	0.949	32.5 ± 0.7	1.057	0.949	4×10^3

Table 2

T	S (calamitic)	S (discotic)
1.00	0.749 ± 0.001	0.783±0.0004
1.25	0.696 ± 0.003	-
1.50	0.623 ± 0.003	0.747±0.002

References

1. Chandrasekhar, S., *Liquid Crystals*, Cambridge University Press, Cambridge, 1992.
2. DeGennes, P. G. and Prost, J., *The Physics of Liquid Crystals*, Clarendon Press, Oxford, 1993.
3. G. W. Stewart, J. Chem. Phys., 1936, **4**, 231
4. D. O. Holland and G. W. Stewart, Phys. Rev., 1937, **51**, 62
5. G. W. Stewart, D. O. Holland and L. M. Reynolds, Phys. Rev., 1940, **58**, 174
6. G. W. Stewart, 1946, **69**, 51
7. J. J. C. Picot and A. G. Fredrickson, I and EC Fundamentals, 1968, **1**, 84
8. J. Fisher and A. G. Fredrickson, Mol. Cryst. and Liq. Cryst., 1969, **6**, 255
9. M. N. Patharkar, V. S. V. Rajan and J. J. C. Picot, Mol. Cryst. Liq. Cryst., 1971, **15**, 225
10. P. K. Currie, Rheologica acta, 1973, **12**, 165
11. P. J. Barratt, Liquid Crystals, 1989, **4**, 223
12. E. Plaut and W. Pesch, Phys. Rev. E, 1999, **59**, 1747
13. S. Weiss and G. Ahlers, J. Fluid Mech., 2013, **737**, 308
14. S. Sarman, J. Chem. Phys., 1994, **101**, 480
15. Evans, D. J., and Morriss, G. P., *Statistical Mechanics of Nonequilibrium Liquids*, Academic Press, London, 1990
16. De Groot, S. R. and Mazur, P., *Nonequilibrium Thermodynamics*, Dover, New York, 1984
17. T. Ikeshoji and B. Hafskjold, Molecular Physics, 1994, **81**, 251
18. D. J. Evans, Mol. Phys., 1977, **34**, 317
19. S. Sarman, D. J. Evans and P. T. Cummings, Phys. Rep., 1998, **305**, 1
20. D. J. Evans, Mol. Phys., 1993, **80**, 221
21. J. H. Irving and J. G. Kirkwood, J. Chem. Phys., 1950, **18**, 817
22. Evans, D. J. and Murad, S., Mol. Phys., 1989, **68**, 1219.
23 J. G. Gay and B. J. Berne, J. Chem. Phys., 1981, **74**, 3316.
24. Bates, M. A. and Luckhurst, G. R., J. Chem. Phys., 1996, **104**, 6696.

25. C. Zannoni, J. Mater. Chem., 2001, **11**, 2637

26. A. Baranyai and D. J. Evans, Mol. Phys., 1990, **70,** 53

27. S. Sarman and A. Laaksonen, J. Chem. Phys., 2009, **131**, 144904

28. S. Sarman and A. Laaksonen, J. Comput. Theor. Nanosci., 2011, **8**, 1081

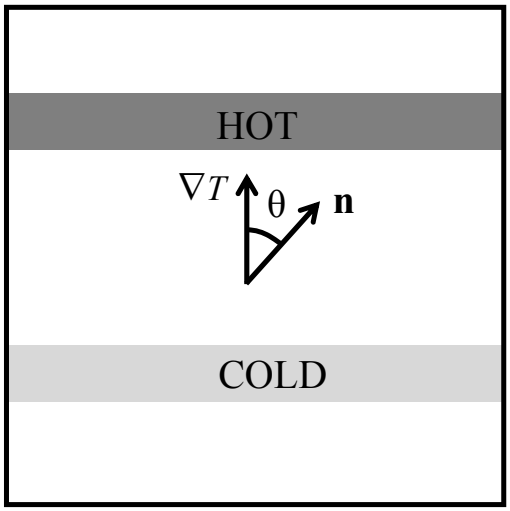

Fig. 1

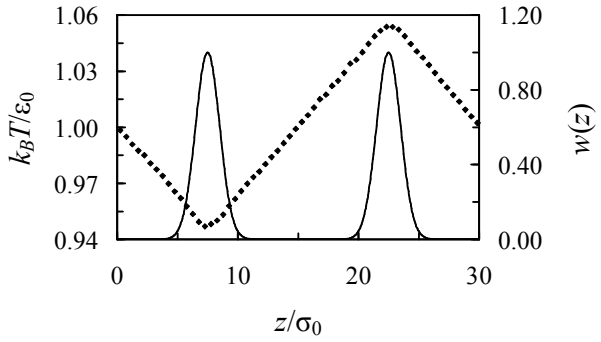

Fig. 2

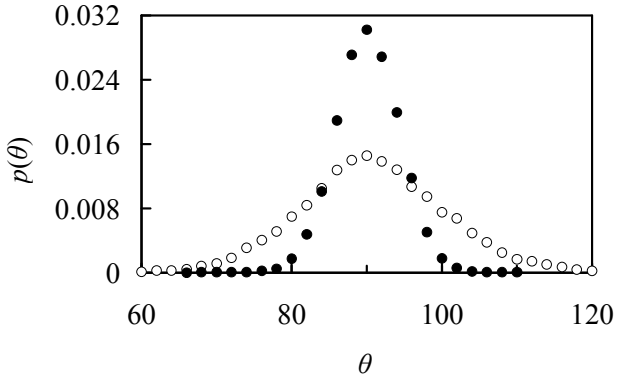

Fig. 3

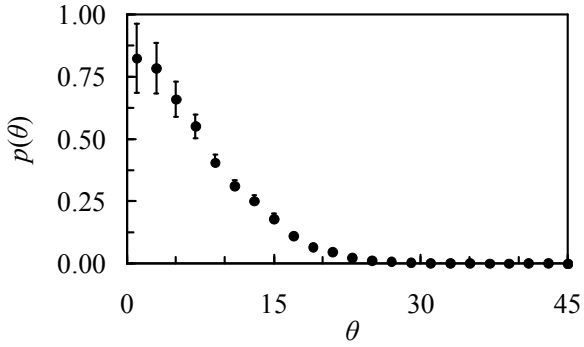

Fig. 4

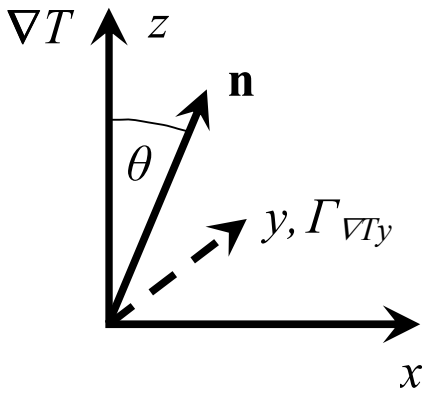

Fig. 5

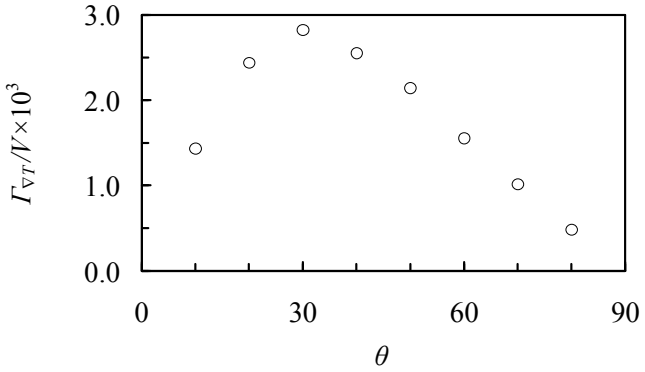

Fig. 6a

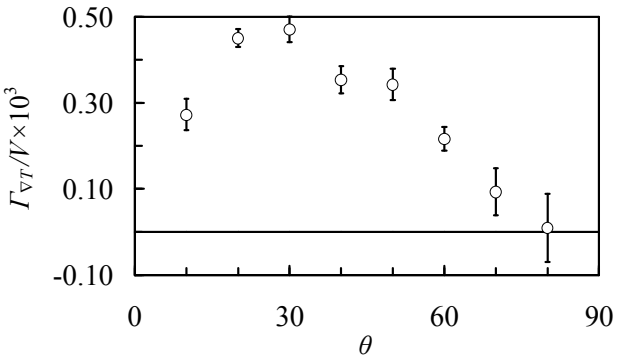

Fig. 6b

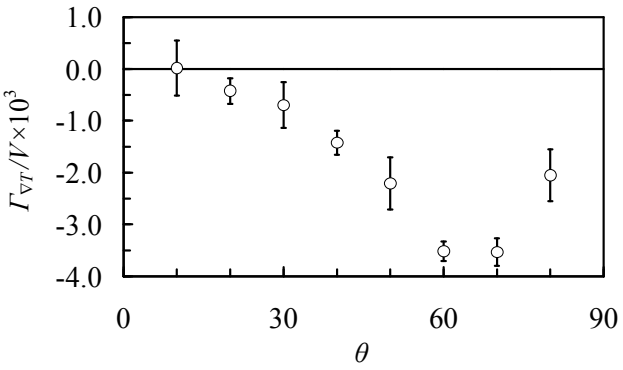

Fig. 7

Colour graphics

Nematic liquid crystal oriented by a temperature gradient